X-ray photoelectron spectroscopy analysis of tribostressed samples in the presence of ZnDTP: a combinatorial approach

Michael Eglin[a,*], Antonella Rossi[a,b] and Nicholas D. Spencer[a]

[a]*Laboratory for Surface Science and Technology, Department of Materials, Swiss Federal Institute of Technology, ETH Zürich, CH-8092 Zürich, Switzerland*

[b]*Department of Inorganic and Analytical Chemistry, University of Cagliari, INSTM, Cagliari, Italy*

Received 15 December 2002; accepted 12 April 2003

The influence of load on the chemistry of tribofilms formed on a steel surface in solution of pure di-isopropyl zinc dithiophosphate (i-ZnDTP) in *n*-decane has been investigated by means of a combinatorial tribological experiment involving X-ray photoelectron spectroscopy. The experiment consisted of the preparation of a set of spatially separated areas, produced under various tribological test conditions, and the subsequent spectroscopic probing of the chemical composition of the tribofilm. The experiment was carried out at room temperature under boundary-lubrication conditions and revealed a physically adsorbed layer of the additive in the non-contact area and a thin (ca. 5 nm), inhomogeneous phosphate film covering the tribostressed areas. The total amount of phosphate present in the tribostressed area was found to increase with increasing load. In the contact areas, iron oxides and metal sulfides have also been detected.

KEY WORDS: boundary lubrication, isopropyl ZnDTP, X-ray photoelectron spectroscopy, combinatorial tribochemistry

1. Introduction

In a previous paper [1] we presented tribological results obtained by applying a new combinatorial approach to the study of the interaction of a lubricant additive with tribostressed surfaces. In this paper, the combinatorial approach has been combined with imaging XPS (i-XPS) and small-area XPS (SAXPS) in order to characterize the tribochemistry of an additive interacting with steel surfaces. A model compound, di-isopropyl zinc dithiophosphate (i-ZnDTP), was chosen for investigation, since zinc dialkyl dithiophosphates (ZnDTPs) have been the most prominent antiwear additives in lubricating oils for over forty years [2]. ZnDTP was originally added to lubricating oil as an antioxidant, but it was rapidly discovered that it also functioned as a highly effective antiwear and extreme-pressure (EP) additive, and it is an essential ingredient in the vast majority of current commercial lubricant formulations [3]. Although it is one of the most studied additives, its outstanding properties in antiwear film formation are still not completely understood. An important role of ZnDTP in such lubricants is to act as an antiwear agent by forming a protective film on the rubbing surfaces [4]. Much information has been published on the thickness, structure and chemistry of the films as well as the mechanism of film formation under tribological stress. The ability of ZnDTP to function in different ways depending on the nature and severity of the tribological conditions may be one of the reasons for the often divergent results reported in the literature. Several authors have proposed a layered structure of a few 100 nm thickness, consisting of iron oxides, sulfides and poly (thio) phosphates or alkylphosphates [3,5–7]. It has also been reported that in the mild-wear regime (0.26 GPa contact pressure, 50 Hz, 15 mm stroke length, 60 °C), the wear-reducing action of ZnDTP is mainly due to the rheological properties of the thermally formed polyphosphate glassy films, whereas under severe conditions (1 GPa contact pressure, 0.5 m/s, 100 °C), short-chain mixed iron/zinc phosphate glasses are formed [5].

As far as the film-formation mechanism is concerned, it is generally agreed that the molecule interacts only weakly with the steel surface at room temperature, starting to decompose around 50 °C on iron substrate [8]. It has been suggested that upon reaching 100 °C ZnDTP undergoes a thermally activated rearrangement in solution to form a linkage isomer (LI-ZnDTP) [3,7,9] as a precursor to the formation of a long-chain glassy polyphosphate and poly-thiophosphate film on the surface. Due to the thermally activated formation of the LI-ZnDTP, as well as the thermo-oxidative processes and wear involved in the film formation, the composition of the generated films changes with temperature [3,6]. Without thermal activation, only very thin films are formed in the tribological contact, whereas at higher temperatures the film thickness increases [10]. Recent work from our laboratory using *in situ* attenuated total reflection infrared spectroscopy (ATR FT-IR) has allowed changes in the additive

* To whom correspondence should be addressed. E-mail: michael.eglin@mat.ethz.ch

1023-8883/03/1000–0199/0 © 2003 Plenum Publishing Corporation

chemistry due to adsorption, as well as reaction film growth, to be followed as a function of temperature and time [11,12]. The reported ATR FT-IR spectra confirm thermal decomposition of ZnDTP with the formation of P–O–P species at 150 °C, while a short-chain phosphate film has been detected on the iron surface following tribotests at the same temperature [13].

The detailed chemistry of these films is still controversial: older works based on elemental analysis with SEM-EDX showed that the film contained Zn, S, P, C and O [14]. XPS [15] and AES [16,17] have also been used to provide chemical differentiation for the different elements; P was claimed to be present as a phosphate and S as a sulfide, the corresponding cation being zinc or iron. XANES spectroscopy revealed that the chemical nature of P and S in the tribofilms was different from that of the pure ZnDTP substances and depends on the alkyl group used in ZnDTP [18]. With isopropyl ZnDTP, phosphorus is found to correspond closely to metaphosphate (polyphosphate with a cyclic structure) whereas with *n*-butyl ZnDTP pyrophosphates are found. This is important when discussing the results obtained from commercial ZnDTP, which often consist of a blend of ZnDTP molecules containing different alkyl groups [3].

A detailed analysis of the high-resolution XP spectra allows further information to be obtained. From the oxygen O(1s) signal, not only oxide and phosphate can be distinguished but, due to the substantial chemical shifts in the signals of the phosphate group, non-bridging oxygen (NBO: PO^-, POH, P=O) at 532.2± 0.2 eV and bridging oxygen (BO: P–O–P) at 534.4± 0.2 eV can be differentiated [19–22], allowing the chain length of polyphosphates to be estimated [21,23]. The phosphorus P(2p) signal has been used to distinguish between orthophosphates, metaphosphates and polyphosphates [21,22]. After thermal decomposition of ZnDTP on an iron surface, zinc polyphosphates could be detected, whereas only simple phosphates were detectable after tribological testing at the same temperature [22].

The difficulty in assignment of chemical state based on binding energies alone should not be underestimated. While the sulfur S(2p) signal provides information about the oxidation state of sulfur, and thus sulfates and sulfide can be readily distinguished, it is much more difficult to identify the cation from the binding energy of the S(2p) peak alone. The chemical state of zinc cannot be identified from the Zn(2p) signal due to the very small chemical shifts between zinc signals in ZnO, ZnS or Zn-polyphosphates. However, the Zn(LMM) X-ray excited Auger signal shows a stronger dependency on the chemical environment [15,24]. It has been shown, for example, that a two-dimensional chemical-state plot of zinc can effectively distinguish between zinc sulfide and oxide [25]. This method can also be extended to differentiate between zinc phosphate or polyphosphate in the contact and non-contact areas of tribostressed surfaces [26].

Most of the published surface-analytical studies of ZnDTP have been based on the analysis of several mm^2, and thus an average chemical composition has been obtained, despite the well-known fact that the films at the micron level are inhomogeneous and ''patchy'' as revealed by SEM [27] and AFM [28]. Therefore, imaging spectroscopic methods were used to investigate films formed during tribological contact in the presence of lubricant additives. Imaging XPS provides quantitative elemental and chemical state information with a lateral resolution in the submillimeter range [29–31]. Synchrotron-based photoemission electron microscopy (PEEM) offers higher lateral resolution (micrometer range) with elemental and chemical state information [32], but it is less quantitative. Scanning Auger Microscopy allows elemental mapping with a lateral resolution in the submicrometer range [16,33], but chemical-state-induced Auger shifts are not easy to interpret, even though recent results suggest that it is possible to distinguish between oxygen in oxides and in phosphates [34].

So far, the imaging possibilities of these surface-analytical methods were applied to relatively simple systems, e.g. traditional pin-on-disk tests [32]. To gain a better insight into the possible tribochemical reactions of a given lubricant-additive system depending on the applied tribological conditions, imaging methods can be used in combination with a combinatorial experiment [1]. A combinatorial sample is produced by systematically varying the parameters defining the tribological stress, spatially separated on a single sample. Imaging spectroscopic methods are then used to analyze the combinatorial sample and extract spectroscopic information for the various conditions applied. One of the parameters studied is the load dependence of the film structure [6,10,35]. It has been reported that higher loads increase the ZnDTP decomposition rate and lead to long-chain polyphosphates [6]. The film thickness of the tribofilm increases to a maximum value with increasing load and may break down upon further increase [10]. The following describes an investigation into the load dependence of the chemical composition of the tribofilms formed in a 1 wt.% solution of i-ZnDTP in decane. These have been analyzed by means of i-XPS and SAXPS.

2. Experimental

2.1. Sample preparation

Steel disks (AISI 52100) were ground using P120, P600 (in tap water) and P1200, P2500 (in ethanol (p.a.)) silicon carbide paper, and polished in ethanol using 3, 1, and 1/4 μm diamond paste. The surface roughness (Ra) was measured by interferometric methods and always found to be less than 10 nm. After polishing, the samples

were kept for three days in a desiccator to allow an oxide film to grow and thus to provide a reproducible surface composition. The samples were ultrasonically cleaned in ethanol and analyzed for surface contamination by XPS immediately prior to tribotesting. Commercial 4 mm ball-bearing balls (AISI 52100) were used as a counterface. They were ultrasonically cleaned in ethanol before the tribotest.

2.2. Tribotest

The steel disk was tribostressed in a ball-on-disk setup with a CETR UMT-2 tribometer (Center for Tribology, Inc., Campbell, CA, USA). This tribometer allows load, rotational velocity and duration of the tribotest to be programmed. The tribometer is equipped with a load cell with a maximum capacity of 5 N and a resolution of ±5 mN in two axes (normal load and friction force). Normal load is applied from the carriage via a spring. The normal load is constantly monitored and adjusted via a feedback loop moving the carriage up or down. The spring constant was determined to be 2.7 N/mm in the z-direction and 5.7 N/mm in the y-direction (friction force). The instrument is capable of recording normal load, friction force, rotational position of the disk and the y-position of the carriage versus time.

As a lubricant, a 1 wt% solution of di-isopropyl zinc dithiophosphate (i-ZnDTP) in decane was used. To dissolve the additive in the lubricant, the solution was stirred at 60 °C for 30 min. The tests were carried out at room temperature (24 ± 0.5 °C). The relative humidity of the air was recorded during each test and was determined to be between 22 and 38%. Decane has a boiling point of 174 °C. This fact hindered investigations at higher temperatures due to problems with evaporation.

Prior to the actual tests, the ball was run in at a load of 5 N with a speed of 31.4 mm/min for 2 h outside the region to be analyzed, in order to create a flat spot on the ball, defining the apparent contact area in the tribotest that followed.

A full tribotest consisted of the formation of five, individual, concentric test areas, each corresponding to a different load. The relative velocity between the ball and the disk surface was kept constant at 31.4 mm/min for all the tribostressed areas, while the load was changed from 0.05 to 5 N between the tested areas. The apparent contact pressure was calculated to be 2.8–280 MPa using the applied load and the apparent contact area defined by the flat spot produced during the running in. The number of turns of the ball on the disk was kept constant for each load, in order to impart comparable tribostress. The ball was moved radially by 25 μm after each fifth turn. Thus, for each load, 11 overlapping wear tracks formed a tribostressed annulus with a width of >250 μm. This allows XPS analysis to be performed completely within the tribostressed area. After the tribotest, the samples were cleaned in cyclohexane in an ultrasonic bath for 30 s and dried under an argon stream before being introduced into the analysis chamber.

2.3. XPS

The XPS analyses were performed on a PHI 5700 system with an Omni Focus IV lens system. The residual pressure in the spectrometer during the data acquisition was always below 5×10^{-7} Pa. The X-ray source was Al Kα (1486.6 eV) run at 350 W. The diameter of the analyzed area was 120 μm. The spectrometer was operated in the fixed analyzer transmission (FAT) mode with a pass energy of 46.95 eV (full width of half-maximum (FWHM) for $Ag(3d_{5/2}) = 1.1$ eV). The instrument was calibrated using the spectral lines of $Au(4f_{7/2})$ and $Cu(2p_{3/2})$ at 83.95 eV and 932.63 eV, respectively [36]. $Ag(3d_{5/2})$ and Cu(LMM) peak energies at 368.22 eV and 567.96 eV respectively, were used to verify the linearity of the binding-energy scale. The accuracy was ±0.05 eV.

Spectroscopic maps were acquired using the imaging capabilities of the Omni Focus IV lens system. The analyzed spot (diameter 120 μm) was electrostatically rastered over the sample (typically 64×64 pixels, 2×2 mm). For each pixel a full spectrum of the selected energy region was acquired. The acquired images were processed with the PHI Multipak (V6.0) software. Spectra can be extracted from the map by selecting a region of interest and can be used to reconstruct "chemical-state maps" with the linear-least-squares (LLS) routine. The correlation between the extracted spectra and the spectrum at each pixel generates a new map, which shows regions having similar chemical states of a given element.

From these maps, areas of interest were determined and analyzed by SAXPS. For curve fitting, CASA XPS software (V2.0, CASA Software Ltd, UK) was used. The spectra were resolved into their components after an integrated Shirley background subtraction. Curve-fitting parameters (FWHM and Gaussian/Lorenzian ratio) were determined from reference spectra. The spectra were fitted with Gaussian/Lorenzian peaks, keeping the FWHM and the Gaussian/Lorenzian ratio constant and fitting the energy of the peaks and their heights using a LLS algorithm. Quantitative analysis was performed using the photoionization cross-section according to Scofield [37] and correcting the intensities for the inelastic mean free path, according to Seah and Dench [38], as well as the analyzer transmission function [39]. The accuracy of the measurements was estimated to be ±0.1 for all measurements, unless otherwise stated. The results presented in this paper refer to two independent experiments.

2.4. Auger electron spectroscopy

The Auger mapping was performed on a VG ESCALAB 200 using an electron gun, which allows 2000 Å lateral resolution. The electron beam, of energy of 10 keV (inducing a specimen current of 20 nA), was rastered to produce 128×128 pixel maps, which were recorded on an IBM 486 computer.

The Auger maps were corrected for topographical effects using the (peak-background)/background algorithm.

2.5. Reference compounds

Reference compounds, $FePO_4.nH_2O$, ZnS and ZnO (Aldrich) were pressed into pellets and mounted in a standard PHI sample holder. i-ZnDTP was supplied by Prof. J.M. Martin. The samples were cooled with liquid nitrogen during measurements to reduce outgassing of the compounds. Reference compounds were analyzed by XPS under the same experimental conditions as reported in section 2.3. The results were confirmed by experiments performed with aperture #3 (0.4 mm diameter) and pass energy 23.5 eV with higher energy resolution.

3. Results

3.1. Tribological results

The coefficient of friction (COF) measured during the tribological test is presented in figure 1 as a function of the applied load. The two bars represent two independent samples. The reported COFs are the values averaged over the last full turn of the disk at the particular load. It is assumed that, at this time, a tribological film that is representative for the particular load is formed and thus the COF is a representative value for the applied conditions. The error bars represent the experimental error, calculated from the error propagation of the load-cell resolution. Despite the large experimental error at low loads, a slight decrease in COF can be seen for larger loads.

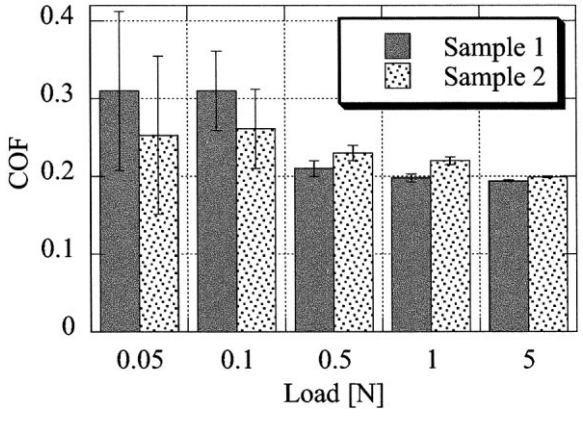

Figure 1. Coefficient of friction (COF) for various loads. The value presented is the average of the last full turn during the test at a particular load. It is assumed that at the end of the test the COF is representative for the protective film formed under the applied conditions. The error bars are calculated using error propagation from the load-cell resolution. The two samples represent two independent experiments.

The morphology of the wear tracks and the ball used for the tribotest were examined with an optical microscope. The ball shows a circular flat spot with a diameter of 150 μm. This spot was produced mainly during the running-in of the ball and defines the apparent contact area during the tests with different loads. In the 5 and 1 N regions the wear tracks are clearly visible on the disk, but for smaller loads no differences can be recognized between the contact and non-contact areas.

3.2. XPS imaging

An O(1s) chemical-state map is shown in figure 2. The chemical-state map is calculated using a linear-least-squares routine, fitting the peak shape of an O(1s) spectrum extracted from a contact region to the spectrum in each pixel of the O(1s) map. The spectrum used to calculate the chemical-state map is similar to that of the 5 N load spectrum shown on the right-hand side of figure 2, and shows a high correlation in the tribostressed areas, forming arcs of a width of 250 μm running across the chemical-state map. The tribostressed areas are labeled according to their applied loads.

On the right-hand side of figure 2, spectra extracted from different areas of the O(1s) map are shown. An increase in the peak intensity can be seen at 531.7 eV as the applied load increases. In the spectra extracted from the non-contact area, a shoulder can be noted at this binding-energy value, which is also present in spectra taken on the steel surface prior to tribotesting.

In order to provide more detail on the chemical species present on the surface, SAXPS analysis was performed in the areas marked with a circle in the O(1s) map.

3.3. Chemical states of the studied elements

3.3.1. Reference compounds

Reference materials, which include the steel surface after mechanical polishing, steel after argon-ion etching, the compounds iron phosphate, iron sulfide, zinc sulfide and zinc oxide, as well as the i-ZnDTP, were analyzed under the same analysis conditions used for obtaining the X-ray photoelectron spectra on the tribostressed samples, in order to derive the curve-fitting parameters to be used for monitoring the changes in the surface chemistry of the tribostressed samples. The peak

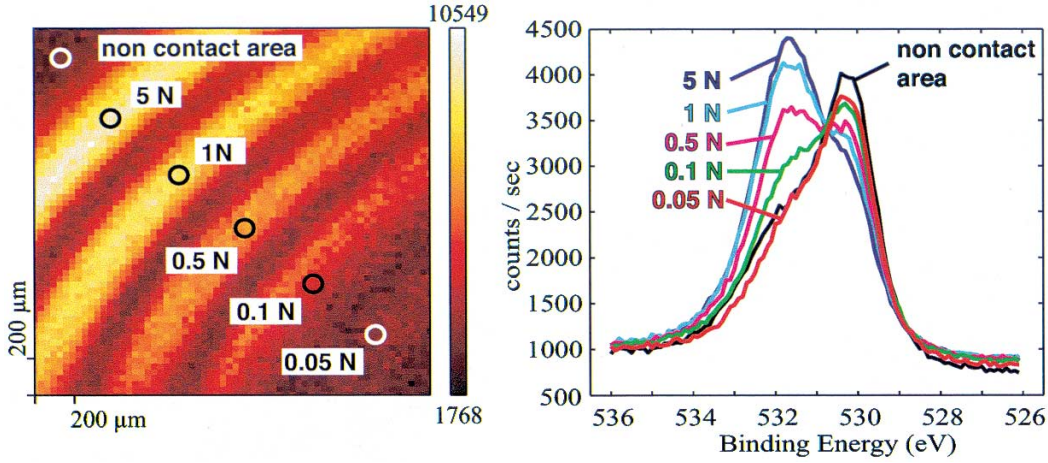

Figure 2. Left-hand side: O(1s) chemical-state map of the five contact areas with the different loads. The map shows the correlation with phosphate-type spectra (extracted from a contact area), and thus the distribution of phosphate-type species. Right-hand side: O(1s) spectra extracted at the points shown in the chemical-state map (circles). The spectra show an increasing peak at 531.7 eV with increasing load. This peak can be assigned to oxygen bound in a phosphate structure.

energies of the main components of the reference compounds are summarized in table 1.

Steel surface after mechanical polishing. The iron Fe($2p_{3/2}$) signal was fitted with Gaussian/Lorenzian peaks and its sum contains the contributions of four signals: The elemental iron Fe(0) signal at 706.8 ± 0.1 eV, Fe(II) at 708.9 ± 0.1 eV (including the Fe(II) shake-up calculated to be 5.5 eV higher in binding energy and 8% of the main peak intensity [40]), Fe(III) at 710.3 ± 0.1 eV and Fe(III) in the oxy-hydroxide layer at 711.9 ± 0.2 eV.

The oxygen signal (figure 3) is composed of three peaks: the first at 530.2 ± 0.1 eV can be assigned to the iron oxide; the second peak at 531.8 ± 0.1 eV is assigned to the iron oxy-hydroxides and the third, at 533.1 ± 0.1 eV, having the lower intensity in comparison with the others, is attributable to adsorbed water.

Steel surface after argon-ion etching. After ion etching, the oxy-hydroxide film, which is always present after mechanical polishing and air exposure, is removed and the spectrum of the iron signal exhibits a peak maximum at 706.8 ± 0.1 eV with an asymmetric tail on the higher-binding-energy side due to multielectron processes.

Iron phosphate. In this case, the P($2p_{3/2}$) signal is found at 133.7 ± 0.1 eV with a FWHM equal to 1.65. The oxygen O(1s) spectrum has been fitted with two Gaussian/Lorenzian curves. The resulting binding energy values are 531.7 ± 0.1 eV for the oxygen in the phosphate group with a FWHM of 1.8 eV and 533.2 ± 0.1 eV due to the water of crystallization. The iron peak has a maximum at 712.2 ± 0.2 eV and has been fitted using a Gaussian–Lorenzian peak with a FWHM of 3.0 ± 0.2 eV.

Zinc sulfide. The most intense zinc signal, Zn($2p_{3/2}$), is found at 1022.1 ± 0.1 eV. The sulfur S2p peak was fitted with the two contributions due to spin-orbit coupling: the binding energy value of the S($2p_{3/2}$) component was equal to 162.0 ± 0.1 eV. Quantitative surface analysis yielded 45 at.% Zn, 55 at.% S.

Table 1
Binding energies of the photoelectron peaks measured in the contact areas (mean value for all loads), the non-contact areas and for the reference compounds. The standard deviation is 0.1 eV for all values listed, except for S $2p_{3/2}$ (see text).

	O 1s (I)	O 1s (II)	O 1s (III)	P $2p_{3/2}$	S $2p_{3/2}$ (I)	S $2p_{3/2}$ (II)	Zn $2p_{3/2}$
Tribostressed samples							
Contact area	530.2	531.6	532.9	133.6	161.9	163.2	1022.3
Non-contact area	530.2	531.7	532.9	133.4	162.0	163.4	1022.3
Reference compounds							
Steel surface	530.2	531.8	533.1				
i-ZnDTP [41]			533.1	133.8	162.8		1022.7
$FePO_4$		531.7	533.2	133.7			
ZnS					162.0		1022.1
ZnO	530.2						1021.3

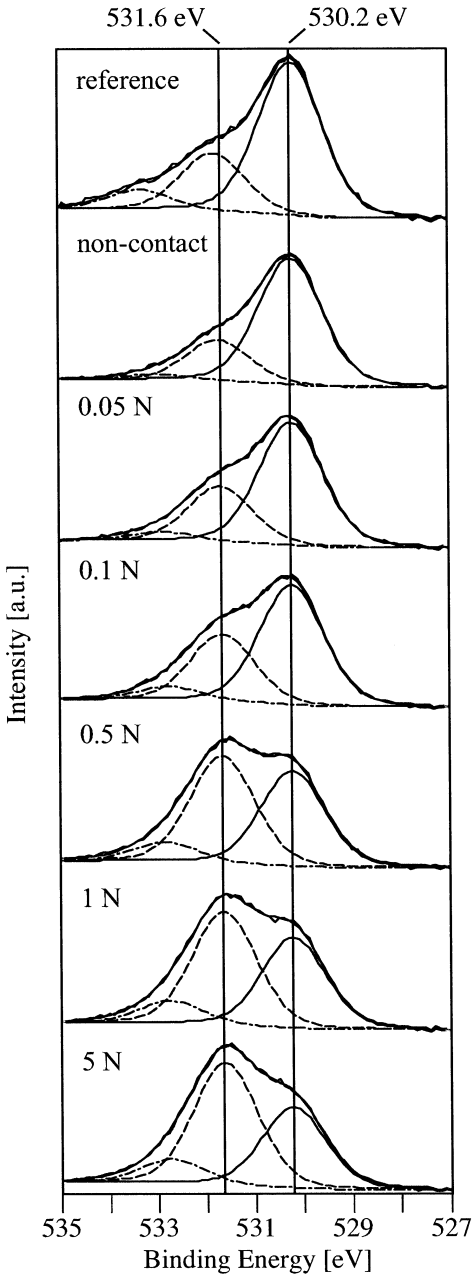

Figure 3. O(1s) peaks of the five different loads together with the non-contact area and the reference spectra of a nascent steel surface. The signals are fitted with three different peaks, a first at 530.2, a second at 531.6 and a third at 532.9 eV.

Zinc oxide. The most intense zinc signal is found at 1021.3 ± 0.1 eV and it exhibits a FWHM of 1.8 ± 0.1 eV; the oxygen O(1s) signal was measured at 530.2 ± 0.1 eV and its FWHM is 1.6 ± 0.1 eV. The quantitative analysis was checked and resulted in excellent agreement with the expected ratio of 1 : 1.

i-ZnDTP [41]. The zinc signal, $Zn(2p_{3/2})$, is found at 1022.7 ± 0.1 eV with a FWHM of 1.9 ± 0.1 eV. The oxygen signal comprises only one signal, found at 533.1 ± 0.1 eV. Phosphorus and sulfur were also fitted, taking into account the splitting and the branching ratio of the two components. $P(2p_{3/2})$ is found at 133.8 eV (FWHM = 1.55 eV) and $S(2p_{3/2})$ at 162.8 eV (FWHM = 1.7 eV). The atomic concentration was found to be 51% C, 15% O, 9% P, 19% S, 5% Zn being in good agreement with the calculated values (52.1% C, 17.4% O, 8.7% P, 17.4% S, 4.4% Zn).

3.3.2. Surface chemistry after tribological tests

High-resolution spectra of the O(1s), S(2p), P(2p), Zn(2p), Zn(3s) and Fe(2p) regions were acquired in the tribostressed areas (see circles in figure 2). For comparison, the non-contact area was analyzed as well. The size of the analyzed area is 120 μm, and thus smaller than the width of the contact region. This ensures that only the tribostressed area is analyzed and thus the spectroscopic information is not averaged with spectral contributions from the non-contact area. In figure 3, the O(1s) peaks for the various loads are displayed. They can be curve-fitted using three peaks. For the curve fitting, a Gaussian/Lorenzian function is used, the G/L ratio was kept fixed at 20% Lorenzian and the FWHM at 1.55 eV while the peak position (binding energy) and peak height were left free to converge. The peak positions do not shift within the experimental error (± 0.1 eV) upon changing the applied load, although they were left free to vary during the curve fitting. The comparison of the spectra collected in the various contact areas corresponding to different applied loads shows that the peak at 531.6 eV increases with increasing load. In the same figure, the O1s spectra of the steel surface immediately prior to tribotesting, together with the oxygen spectra collected in the non-contact area, are also displayed. The binding-energy values of the three components are listed in table 1 with the binding-energy values of the $P(2p_{3/2})$, $S(2p_{3/2})$ and $Zn(2p_{3/2})$ peaks.

The P(2p) and S(2p) peaks were fitted using a doublet, taking into account the theoretical ratio of the spin-orbit coupling (1 : 2). The separations of the two peaks were determined by reference measurements and kept constant for data processing (1.2 eV for sulfur and 0.84 eV for phosphorus). The $P(2p_{3/2})$ is found at 133.6 ± 0.1 eV in the contact regions (independently of the applied load) and 133.4 ± 0.1 eV in the non-contact region.

The FWHM of the S(2p) peak in the contact areas were found to be broader (2.5 eV) than those of the reference spectra (ZnS: 2.2 eV). This suggested that more than one chemical state is present, and thus two doublets were used for the fit. The signal at lower binding energies was found at 161.9 ± 0.1 eV and the second has a peak maximum at 163.2 eV. Due to the low sulfur content in the non-contact area, the S(2p) spectra has a low S/N ratio, which makes it difficult to produce a proper peak fit. These values show a higher standard deviation (± 0.2 eV).

In figure 4, an example of an iron $Fe(2p_{3/2})$ signal collected in an area tribostressed with 1 N is shown, following a Shirley–Sherwood background subtraction.

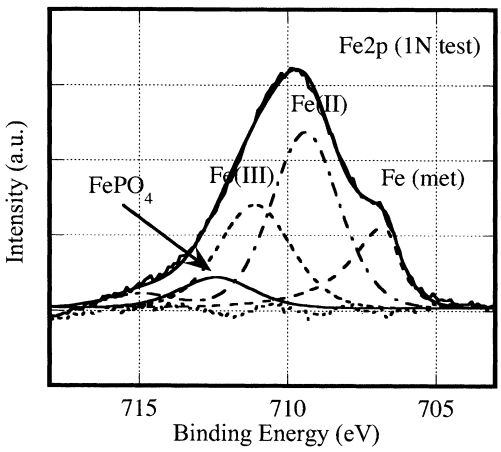

Figure 4. Fe($2p_{3/2}$) spectra collected in an area tribostressed under 1 N load. It is possible to observe a contribution at 712.4 eV, which can be attributed to iron bound to phosphate.

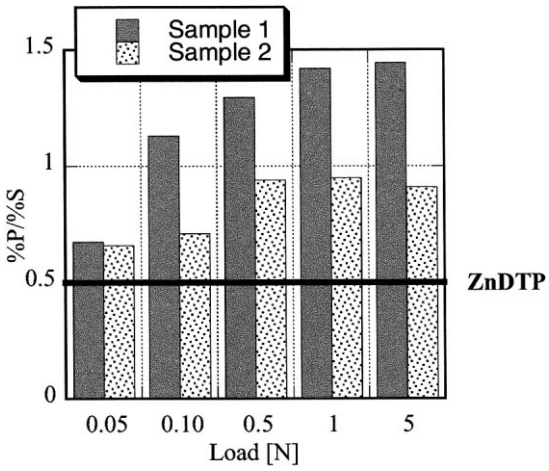

Figure 5. Atomic ratio of P and S for the various loads, calculated using the total area under the P and the S(2p) peaks, corrected with the appropriate sensitivity factors. A substantial increase in P can be seen with increasing load. The two samples represent two independent experiments.

The spectra is quite complex because of the superimposition of the contributions due to the different iron species present in the surface film and the substrate. To extract as much information as possible, a curve-fitting procedure based on the parameters obtained from the reference spectra and leaving only the heights of the curves free to vary was adopted. The contribution to the metallic iron (706.8 eV) is fitted with a tail function in order to avoid an overestimation of the intensity of the other signals. In this case, as for the reference compounds, the iron in the oxidation state (II), found at 709.4 eV, has been fitted together with its satellite (at a binding energy 5.5 eV higher than the main peak), which might interfere with the signals assigned to iron in a phosphate and/or in a hydroxide. The Fe (III) is present at 711.1 eV, whereas the signal at 712.4 eV might be assigned to the iron phosphate signal, according to the results obtained on the reference iron phosphate.

The Zn $2p_{3/2}$ signal was always a Gaussian/Lorenzian symmetric curve: the peak position was found at 1022.3 eV with a FWHM of 1.9 eV, independent of the applied load.

3.4. Composition of the tribofilm

In the following, quantitative results obtained from the measured XPS intensities (areas of the peaks) are presented for two independent samples.

In figure 5, the atomic ratio between phosphorus and sulfur is given for the different analyzed regions. The sum of the spin-orbit contributions (i.e. the total area under each signal) of the sulfur and the phosphorus peaks were used. At higher load the phosphorus-to-sulfur ratio increases. The theoretical ratio between phosphorus and sulfur in i-ZnDTP (0.5) is also given in figure 5. This ratio is close to that found in the non-contact area.

As previously seen in figure 3, the O(1s) peak can be resolved into three different peaks. Figure 6 shows the ratio between the second component of the O(1s) spectra (at 531.6 eV) and the total amount of phosphorus. At high loads the ratio is close to 1 : 4, while at low loads it is higher. The difference between the two samples increases at low loads.

4. Discussion

Most of the work published so far concerning tribofilms formed from ZnDTPs has focused on experiments carried out above 100 °C. It is assumed that these films are a representation for the films produced under real conditions, since ZnDTPs are usually used in applications where elevated temperatures are present. However, although even at room temperature a positive effect of ZnDTP can be observed, very little has been published on the film structure/formation mechanism of

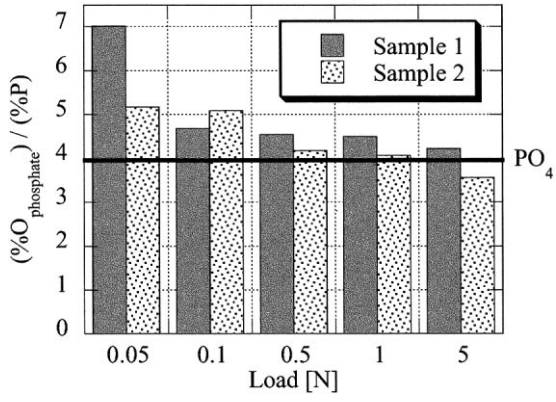

Figure 6. Atomic ratio of O to P for the various loads, calculated using the second component in the O(1s) spectra (at 531.6 eV, see figure 3), attributed to oxygen bound within phosphate and the total P(2p) peak. The two samples represent two independent experiments.

ZnDTP under ambient conditions [10]. Room-temperature measurements are of interest, however, since all machines in which lubricant additives are used start up from room temperature before reaching their operating conditions. It is also frequently the case that the most severe tribological conditions occur during the start-up phase of a machine.

4.1. Tribology and coefficient of friction

Coefficient of friction versus load. The COF values measured in this work are high at all applied loads. This fact substantiates the assumption that the experiments have been carried out in the boundary lubrication regime [42]. Despite the high experimental error in the COF at low loads, a slight decrease in COF can be seen.

Coefficient of friction versus time. A decrease in the COF is detected with time for any given load. This decrease is related to a change in the mechanical properties of the surface film and to a change in the surface composition of the two counterparts. However, with optical microscopy it is difficult to detect wear on the steel surface for applied loads lower than 1 N, although chemical-state maps clearly show the tribostressed areas. This indicates that when an effective additive is employed, it is difficult to observe surface changes with the traditional microscopic techniques but surface analytical methods can contribute to the characterization of the tribofilms. Many such studies have been carried out, but one of the limiting factors is the difficulty of collecting information over a wide-enough range of conditions in order to clarify the mechanism of the film formation. Here, the results of the combinatorial approach provide an insight into the influence of the applied load and other parameters on the chemical composition of the surface film. Differences revealed between the contact and the non-contact regions will also be discussed in the following.

4.2. The surface chemistry of the tribofilm

A chemical-state map (figure 2), reconstructed using the oxygen signal extracted from the contact area, allows the contact area to be distinguished from the non-contact area. Moreover, chemical differences can be detected by looking at the O(1s) signal extracted from areas within the contact regions that were tribostressed with different loads. This allows areas of interest to be selected and analyzed further by SAXPS. The results obtained reveal that in the regions with different loads, no differences in binding energies can be detected. However, differences in the *composition* of the surface film can be readily detected.

Non-contact area: Chemical state and composition. As was pointed out in a recent paper, i-ZnDTP is weakly adsorbed on the non-contact area of the sample surface [31]. The detailed O1s spectra show the main component to be at 530.2 eV with a second, less-intense peak at 531.7 eV, also in the presence of i-ZnDTP. The iron signal remains virtually unaffected in the presence of the second component of the sulfur S($2p_{3/2}$) signal at 163.4 eV, and the shift of the P($2p_{3/2}$) signal to lower binding energies (133.4 eV) (compared with the 133.8 eV found in the pure additive) may suggest that a change in the structure of the i-ZnDTP has occurred. The presence of the metallic signal in the iron spectra at 706.9 eV suggests that the oxy-hydroxide film thickness is less than the escape depth of the photoelectrons (i.e. ≈ 5 nm). Thus it can be concluded that in the non-contact area, an atmospherically formed oxy-hydroxide film is present, together with a very thin physically adsorbed organic layer.

Contact area: Chemical state of the elements and composition. The peak at 530.2 ± 0.1 eV in the O(1s) spectra taken in the contact area of the tribostressed sample arises from iron oxide and is present in all spectra (both on the steel prior to tribotesting and within the contact area for all loads). This shows that there is always some oxide present in the tribofilm. A second oxygen peak is found at 531.6 ± 0.1 eV. The peak position is close, within experimental error, to the position of the iron hydroxides (531.8 ± 0.1 eV) [43] and to the oxygen of iron phosphate (531.7 eV table 1), also in agreement with the literature [44]. The intensity of this second peak increases with applied load, as does the amount of phosphorus found in the contact area. The ratio between the oxygen in this chemical state and the total phosphorus signal, corrected with the appropriate sensitivity factors, was found to be close to 4 : 1 for high loads and increases at low loads (figure 6). The oxygen-to-phosphorus ratio of 4 : 1 would agree with a phosphate structure, while at lower loads some hydroxides might also be present, in addition to the phosphate. The presence of a phosphate might also be supported by the position of the P($2p_{3/2}$) signal found at 133.6 ± 0.1 eV—close to the measured value of the reference iron phosphate at 133.7 eV and 0.2 eV lower than the value found for the free i-ZnDTP (table 1). Reference measurements on surfaces tribostressed in the presence of decane only (no additive) only showed small changes in the relative intensities of the different O1s signal contributions [31]. In this case the ratio of the hydroxide peak to the oxide peak was smaller in the tribostressed area than in the non-contact area, which substantiates our assertion that the O1s peak at 531.6 eV in the contact areas is due to oxygen bound to phosphorus.

As discussed earlier, the binding energies of bridging oxygen (BO) and non-bridging oxygen (NBO) in the O(1s) spectra of a polyphosphate are separated by approximately 1.5 eV [19–22]. The O(1s) peak positions range between 531.6 and 532.6 eV for NBO and 533.1 and 534.1 eV for BO. The differences found in the

literature are probably due to different sample preparation methods. The peak positions of the second O(1s) peak found in the spectra of the contact area are close to the lower values reported in the literature for NBO oxygen. In addition, a small peak can be detected at 532.9 eV, a value which would be rather low for BO. Also, the binding energy of the P($2p_{3/2}$) signal at 133.6 eV is in agreement with literature values for phosphate (133.4–133.8 eV [22,44]) but does not correspond to the literature values for the polyphosphates (134.0–135.0 eV [19–22]). The oxygen-to-phosphorus ratio would also be too high for a polyphosphate. This leads to the conclusion that only phosphates are formed under these experimental conditions at the surface and no polyphosphates are detected. This finding is in agreement with the literature, where it is reported that polyphosphates are formed thermally on the sample and modified with the applied tribological stress [5,12]. The tribological experiments in this work were performed at temperatures where no polyphosphates are thermally formed, leading to a different film composition. It is important to mention that a thin protective film is also formed under these conditions.

The peak position of the component of the S(2p) spectra at 161.9 eV is typical for sulfides. Possible species formed could be zinc sulfide or iron sulfide, but the peak positions of the Fe(2p) and the Zn(2p) signal do not provide any further evidence in this regard. The Zn(LMM) signal (not shown) indicates that the presence of zinc sulfide can be ruled out, and thus zinc might be available to participate in the formation of tribofilms in the phosphate layer. The use of the two-dimensional chemical-state plot, using the Zn(2p) and the Zn(LMM) signal, seems to be a powerful tool to obtain more information on the chemical bonds of zinc [26]. The second component of the sulfur peak at 163.2 eV can be assigned to organosulfur species (e.g. thiols). It can be assumed that after the reaction of the phosphorus present in the ZnDTP molecule to phosphate, part of the sulfur reacts with a metal to form sulfides. The remaining sulfur may react with alkyl chains to form organosulfur species. These species are soluble in the lubricant, and only a small amount would stay adsorbed at the surface or become incorporated in the surface film. This leads to the depletion of S in the contact area in comparison to P.

The XPS iron signals detected in the contact regions are different from those collected on the steel prior to tribotesting: only the component at 706.8 eV is always present. This signal is assigned to the metallic iron of the steel substrate. The differences in binding energies between the Fe(II) and Fe(III) components of the tribofilms and of the natural oxide film can be explained taking into account that in the case of the naturally formed film the aging of the film resulted in a magnetite film, whereas the peak position after tribotest suggests the formation of FeO and maghemite, as has already been found in model alloy studies [45]. Furthermore, the presence of the peak at 712.4 eV suggests at least a partial removal or reaction of the hydroxides, resulting in the formation of iron phosphate: this is also supported by the oxygen-to-phosphorus ratio, which is almost stoichiometric at higher loads (i.e. 4 : 1). Apparently all traces of hydroxides have been removed from the surface, since no hydroxide peak can be detected at 711.9 eV [46].

The approximate film thickness (including a carbon overlayer) can be calculated from the attenuation by the overlying film of the electrons emitted from the metallic iron present in the steel beneath the surface film. It was found to be 5.0 ± 0.2 nm after the 5 N test. This film thickness is significantly smaller than that reported in most other studies. This may be due to the fact that most of these studies have been carried out at temperatures above 80 °C. At these temperatures, but not below, a thick thermal film is formed on the surface. Under the conditions applied in this study, the contact temperature and the tribochemical reaction form a thin phosphate film, but the thermal activation is insufficient to form a thick polyphosphate film.

In order to ascertain the degree of homogeneity of the contact area a Scanning Auger Microscopy O(KLL) map of a 1 N contact area (figure 7) has also been collected on the tribologically stressed samples. It can be seen that the surface composition is not homogenous. The wear tracks are visible, with a regular spacing of 25 μm, arising probably from the 25 μm steps made during the tribotest. In Auger microscopy, it is difficult to distinguish between different chemical states, even though recently the O(KLL) signal has been applied to the chemical-state identification of the species present in a tribofilm [34], while in XPS we have to be aware that we are averaging over the analyzed area. It can be assumed that changes in the distribution of these areas, as reported in the present work, reflect the load dependency of the tribofilm.

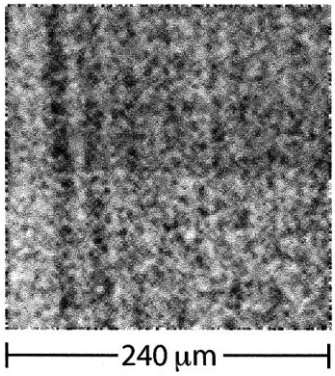

Figure 7. O (KLL) map of an area tribostressed at a load of 1 N. The intensity of the signal shows a periodicity of 25 μm, corresponding to the step size of the tribotest sequence.

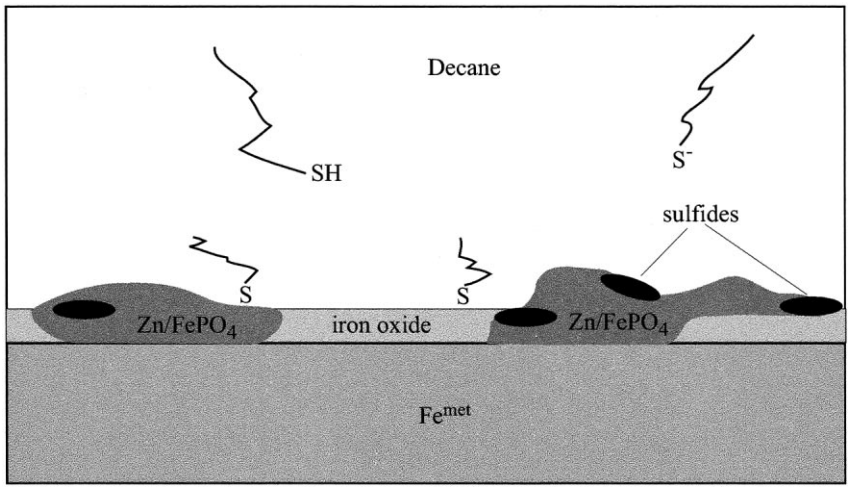

Figure 8. Model of the tribofilm: a mixed iron/zinc phosphate film is formed on the surface. Due to the absence of thermal activation, the protective film is only formed in areas with high tribological stress, occurring predominantly at the asperities. Some iron oxide remains in the less-stressed areas (valleys). Some sulfide is also present. Organosulfur species are formed and remain either dissolved in the oil or adsorbed on the surface. The total film thickness is approximately 5 nm.

4.3. Mechanism of film formation

The proposed mechanism of reaction under these experimental conditions is the following: in the non-contact area a thin, organic layer (including ZnDTP or LI-ZnDTP) is adsorbed. Due to the mechanical and thermal stress during the tribological contact, the adsorbed species and additive molecules from the solution react with the iron oxide to form a protective film. This takes place in the region of highest mechanical and thermal stress. The phosphorus in the ZnDTP reacts with oxygen from the oxide and dissolved oxygen in the oil to form an iron phosphate-containing film, while organosulfur species are released into the solution. Some of these species may react to form sulfides that are incorporated in the film or adsorbed on the surface. The phosphate film is thin (<5 nm) and inhomogeneous. The composition and amount of phosphate film formed on the surface depend on the applied load. The higher the load, the more phosphate is found on the surface. This may be explained by the fact that the higher the applied load, the higher the real contact area. The highest tribological and thermal stresses are found in the real contact area and therefore the tribofilm is formed preferentially in these areas. The amount and the composition of the tribofilm are therefore dependent on the size and the tribological stress in the real contact area. The proposed film structure is shown in figure 8.

5. Conclusion

The results presented here suggest that in the non-contact area, only physical adsorption of ZnDTP takes place on the existing oxide layer. In the contact region, a reaction occurs due to the tribostress and a thin tribofilm is formed. The tribofilm contains iron phosphate and other reaction products, such as sulfides and organosulfur species. The amount and composition of the tribofilm is dependent on load. The phosphate shows a greater increase with increasing applied load than the other species. No polyphosphate could be detected, due to the lack of thermal activation.

The combinatorial approach, especially when combined with imaging surface spectroscopies, has proven itself to be useful in characterizing the lubricant–additive interaction. It allows the tribochemical reaction occurring under a variety of tribological conditions to be characterized, and this approach shows promise as a tool for the screening of new antiwear additives.

Acknowledgments

Financial support of the ETH Zurich and Italian MURST (ex 60% grant to A.R.) is gratefully acknowledged. Prof. J.M. Martin (Ecole Centrale de Lyon, France) is thanked for supplying the i-ZnDTP. Prof. B. Elsener (University of Cagliari, Italy) is thanked for his help with the AES measurements.

References

[1] M. Eglin, A. Rossi and N.D. Spencer, Tribol. Lett. (this issue).
[2] C.H. Bovington, *Chemistry and Technology of Lubricants*, eds. R.M. Mortier and S.T. Orszulik (Blackie and Son, Glasgow and London, 1997).
[3] A.J. Gellman and N.D. Spencer, J. Eng. Tribol. 216 (2002) 443.
[4] D. Klamann, *Lubricants and Related Products* (Verlag Chemie, Weinheim, 1984).
[5] J.M. Martin, Tribol. Lett. 6 (1999) 1.
[6] Z. Yin, M. Kasrai, M. Fuller, G.M. Bancroft, K. Fyfe and K.H. Tan, Wear 202 (1997) 172.
[7] M.L.S. Fuller, M. Kasrai, G.M. Bancroft, K. Fyfe and K.H. Tan, Tribol. Int. 31 (1998) 627.
[8] C.H. Bovington and B. Dacre, ASLE Trans. 27 (1984) 252.
[9] R.B. Jones and R.C. Coy, ASLE Trans. 24 (1981) 91.

[10] S.H. Choa, K.C. Ludema, G.E. Potter, B.M. Dekoven, T.A. Morgan and K.K. Kar, Wear 177 (1994) 33.
[11] F.M. Piras, *In situ* Attenuated Total Reflection Tribometry. PhD Thesis, presented at the Department of Materials, ETH Zürich, 2002.
[12] F.M. Piras, A. Rossi and N.D. Spencer, in: *Proceedings of the 28th Leeds–Lyon Symposium on Tribology*, eds. D. Dowson *et al.*, Vienna, 2002, p. 199.
[13] F.M. Piras, A. Rossi and N.D. Spencer, Langmuir 18 (2002) 6606.
[14] J.S. Sheasby, T.A. Caughlin, A.G. Blahey and K.F. Laycock, Tribol. Int. 23 (1990) 301.
[15] R.J. Bird and G.D. Galvin, Wear 37 (1976) 143.
[16] T.P. Debies and W.G. Johnston, ASLE Trans. 23 (1980) 289.
[17] S. Jahanmir, J. Tribol. Trans. ASME 109 (1987) 577.
[18] Z.F. Yin, M. Kasrai, G.M. Bancroft, K.F. Laycock and K.H. Tan, Tribol. Int. 26 (1993) 383.
[19] E.C. Onyiriuka, J. Non-Crystal. Solids 163 (1993) 268.
[20] R.K. Brow, J. Non-Crystal. Solids 194 (1996) 267.
[21] M. Kasrai, M.L.S. Fuller, M. Scaini, Z. Yin, R.W. Brunner, G.M. Bancroft, M.E. Fleet, K. Fyfe and K.H. Tan, in: *Proceedings of the 21st Leeds–Lyon Symposium on Tribology*, eds. D. Dowson *et al.* Leeds, 1994, p. 659.
[22] F.M. Piras, A. Rossi and N.D. Spencer, Tribol. Lett. (in press) (2003).
[23] R. Gresch, W. Müller-Warmuth and H. Dutz, J. Non-Crystal. Solids 34 (1979) 127.
[24] S.W. Gaarenstroom and N. Winograd, J. Chem. Phys. 67 (1977) 3500.
[25] C.D. Wagner, L.H. Gale and R.H. Raymond, Anal. Chem. 51 (1979) 466.
[26] A. Rossi, K. Matsumoto, M. Eglin, F.M. Piras and N.D. Spencer, in preparation.
[27] J.S. Sheasby and Z. Nisenholz, Tribol. Trans. 36 (1993) 741.
[28] J.F. Graham, C. McCague and P.R. Norton, Tribol. Lett. 6 (1999) 149.
[29] N.D. Spencer, in: *Proceedings of the JAST Tribology Conference, Tokyo*, 1998, p. 396.
[30] F.M. Piras, A. Rossi and N.D. Spencer, submitted to Surf. Interface Anal. (2003).
[31] M. Eglin, A. Rossi and N.D. Spencer, in: *Proceedings of the 28th Leeds–Lyon Symposium* on Tribology, eds. D. Dowson *et al.* Vienna, 2002, p. 49.
[32] G.W. Canning, M.L.S. Fuller, G.M. Bancroft, M. Kasrai, J.N. Cutler, G. De Stasio and B. Gilbert, Tribol. Lett. 6 (1999) 159.
[33] T. Le Mogne, J.M. Martin and C. Grossiord, Tribol. Series 36 (1999) 413.
[34] J.M. Martin, C. Grossiord, T. Le Mogne, S. Bec and A. Tonck, Tribol. Int. 34 (2001) 523.
[35] W.A. Glaeser, D. Baer and M. Engelhardt, Wear 162–164 (1993) 132.
[36] M.P. Seah, Surf. Interface Anal. 31 (2001) 721.
[37] J.H. Scofield, J. Elect. Spect. Rel. Phen. (1976) 129.
[38] M.P. Seah and W.A. Dench, Surf. Interface Anal. 1 (1979) 2.
[39] K. Berresheim, M. Matternklosson and M. Wilmers, Fresenius J. Anal. Chem. 341 (1991) 121.
[40] R.P. Gupta and S.K. Sen, Phys. Rev. B 12 (1975) 15.
[41] M. Eglin, A. Rossi, F.M. Piras and N.D. Spencer, Surface Sci. Spectra 8 (2001) 97.
[42] G.W. Stachowiak and A.W. Batchelor, *Engineering Tribology* (Butterworth–Heinemann, Boston, 2001).
[43] A. Rossi and B. Elsener, Mat. Sci. Forum 185–188 (1995) 337.
[44] D. Schuetzle, R.O. Carter, J. Shyu, R.A. Dickie, J. Holubka and N.S. McIntyre, Appl. Spect. 40 (1986) 641.
[45] A. Rossi, B. Elsener and G. Puddu, *Materials and Corrosion* (in press) (2002).
[46] N.S. McIntyre and D.G. Zetaruk, Anal. Chem. 49 (1977) 1521.